$^{17}O(\vec{d},t)^{16}O$ at 89 MeV; j dependence and particle-hole matrix elements

Swapan K. Saha, W. W. Daehnick, S. A. Dytman, P. C. Li, and J. G. Hardie
Department of Physics, University of Pittsburgh, Pittsburgh, Pennsylvania 15260

G. P. A. Berg, C. C. Foster, W. P. Jones, D. W. Miller, and E. J. Stephenson
Indiana University Cyclotron Facility, Bloomington, Indiana 47405
(Received 16 April 1990)

Differential cross sections and analyzing powers were measured for $^{17}O(\vec{d},t)^{16}O$ with polarized deuterons of 89 MeV. States of ^{16}O up to 22.89 MeV excitation energy have been studied with an overall resolution of 60 keV. Discrimination between analyzing powers (A_y) for different j transfers was found to be very good. The unique $A_y(\theta)$ shapes were used to deduce $p_{1/2}$-$p_{3/2}$ mixing ratios for those levels where it was significant. We find unexpectedly strong mixing for the 6.130 MeV, 3^-, and 8.872 MeV, 2^-, levels. Exact finite-range distorted-wave Born approximation calculations were used to identify l transfers and to extract spectroscopic strengths. Up to 23 MeV excitation, pickup strength is dominated by $1p$ transfer; less than 2% of the observed particle-hole strength results from $2s$, $1d$, or $1f$ transfer. Twelve particle-hole matrix elements for $(p_{1/2}^{-1}d_{5/2})$ and $(p_{3/2}^{-1}d_{5/2})$ configurations have been deduced. Comparison with previous work shows general agreement except for the $T=0, J^\pi=3^-$ term.

I. INTRODUCTION

Accurate calculations of nuclear wave functions in the shell-model framework depend on the inclusion of all relevant configurations and the reliability of the two-body residual interaction used. One-nucleon pickup reactions from "single-nucleon" targets are a familiar way to experimentally check or extract the proper matrix elements for the two-body residual interaction. The extracted matrix elements are quite reliable, provided all significant components of configuration with given J^π and T are found and the amount of configuration mixing, if any, for a given state is known or deducible.

In order to satisfy these conditions one has to search to high enough excitation energy with good resolution. Measurements of analyzing powers (A_y) provide a practical way to extract configuration mixing, because it has been found[1-3] that A_y is very sensitive to the total angular momentum j transferred.

^{17}O is a suitable nucleus for studying the particle-hole residual interaction for the $(1p_{1/2}^{-1}1d_{5/2})$ and $(1p_{3/2}^{-1}1d_{5/2})$ configurations through the one-nucleon pickup reaction. Several such experiments have been reported.[1,4-8] However, in earlier $^{17}O(d,t)$ or $^{17}O(^3He,\alpha)$ experiments the resolution was only 90–120 keV, and just a fraction of the $J^\pi=1^-$ $(1p_{3/2}^{-1}1d_{5/2})$ strength was located. Shell-model calculations for ^{16}O, published in Refs. 9 and 10, predict some $p_{3/2}$ strength as high as 24.10 MeV. Calculations of Ref. 9 suggest very small spectroscopic strengths (0.13) for the shell model "forbidden" transitions, but recent shell-model calculations by Glaudemans[10] in an enlarged model space including $2\hbar\omega$ excitations suggest large $2s$-$1d$ configuration admixtures for all $A=4$–16 nuclei.

In the present $^{17}O(\vec{d},t)^{16}O$ experiment we used the high resolution K600 spectrograph at the Indiana University Cyclotron Facility (IUCF) and a 89-MeV deuteron beam. Our goal was to search for the missing $p_{3/2}$ strength, especially for $J^\pi=1^-$ strength, to discriminate between different j transfers through the measurements of A_y, and to look for the existence of $s-d$ strength at high excitation energy. We searched up to 25 MeV excitation in ^{16}O with an overall resolution of 60 keV.

The experimental procedure is described in Sec. II. Experimental results and uncertainties are given in Sec. III. Section IV describes the finite-range distorted-wave Born approximation (DWBA) calculations used for extracting the spectroscopic strengths. It also describes the procedure used to unfold j mixing for those states where j mixing was observed. Individual levels are discussed in Sec. V. The spectroscopic factors and the deduction of the empirical particle-hole matrix elements are discussed in Sec. VI.

II. EXPERIMENTAL PROCEDURE

The present $^{17}O(\vec{d},t)^{16}O$ experiment was performed at the Indiana University Cyclotron Facility (IUCF) with polarized deuterons of energy 89.1±0.1 MeV. The vector beam polarization (P_y) was checked at the beginning and at the end of the data taking and was found to be nearly constant at $P\uparrow=0.515$ and $P\downarrow=-0.544$. The tensor component of the beam averaged $P_{yy}=0.025$ for the two spin states, and should have a negligible impact on the cross-section normalization. The vector polarization was deduced from the asymmetry of protons ejected from the $^3He(\vec{d},p)^4He$ reaction, measured near 7.1 MeV with a gas cell located in the beam line between the injector and main stage cyclotrons. The helium polarimeter

was calibrated for vector polarization based on the properties of the RF transitions in an atomic beam source and the $A_{yy}=-2$ tensor analyzing power of the $^{16}O(\vec{d},\alpha)^{14}N^*$ reaction leading to the 0^+ state of ^{14}N at 2.313 MeV. The details of this procedure are summarized in Ref. 11. The spin states of the beam were controlled remotely and were flipped twice per minute in order to reduce systematic errors.

The reaction products were studied by using the new high-resolution K600 spectrometer. The spectrograph aperture had a horizontal opening angle of $\Delta\theta=3.27°$. An external Faraday cup located ~7.9 m downstream from the target was used for all measurements, which were taken at 17.5°, 25°, 35°, 40°, and 45°. At these angles A_y is large and differences for $p_{1/2}$ and $p_{3/2}$ transfers are most distinct.[3]

The K600 detector system included two vertical-drift chambers (VDC) for determining the horizontal positions of the ejectiles at the focal plane, followed by two plastic scintillators (0.32 cm and 1.27 cm thick) serving as a timing reference for the drift time measurement and as a particle identifier. Each VDC consisted of 160 sense wires with two guard wires placed between pairs of sense wires with each wire separated from its neighbors by 2 mm. The VDC's were operated at 4900 V cathode-plane bias and with grounded guard and sense wires. Two magnetic field settings had to be used to cover excitation energies of up to about 25 MeV. Good energy resolution was achieved by optimizing focusing and dispersion matching conditions on the target with a slit mounted very close to the target, as discussed in detail in Ref. 12. The overall resolution for this experiment was 60 keV.

Three different SiO_2 targets were used. One of these targets, a nominal thickness of 2.75 mg/cm^2, was enriched to 61% in ^{17}O. Another target, a nominal thickness of 4.6 mg/cm^2, contained oxygen enriched to 95% in ^{18}O, and the third one, a thickness of 2.4 mg/cm^2, contained natural oxygen. The ^{17}O and ^{16}O targets were surrounded by a graphite frame. Data were taken with the ^{18}O and ^{16}O targets to identify the $^{18}O(\vec{d},t)^{17}O$ and $^{16}O(\vec{d},t)^{15}O$ peaks that appear together with the $^{17}O(\vec{d},t)^{16}O$ peaks from the ^{17}O enriched target.

The data acquisition program used was "Q" (developed at Los Alamos National Laboratory, Los Alamos, New Mexico) running on a VAX 11-750 computer. About 85% of the particles identified as tritons met the conditions for a "good" event and were histogrammed. Data were accumulated on magnetic tapes in event-by-event mode.

III. EXPERIMENTAL RESULTS

Figure 1 shows the $^{17}O(\vec{d},t)^{16}O$ spectrum at $\theta_{lab}=17.5°$ taken with a SiO_2 target. Impurities seen are from the ^{16}O and ^{18}O admixtures which produced ^{15}O and ^{17}O peaks, respectively. In addition (kinematically broadened) ^{27}Si peaks are also present. We identified 32 peaks of ^{16}O up to an excitation energy of about 23 MeV. The triton spectra were measured up to about 25 MeV; but above 23 MeV, poor statistics and ^{11}C peaks arising from the beam halo striking the graphite frame made it impossible to identify any ^{16}O peaks.

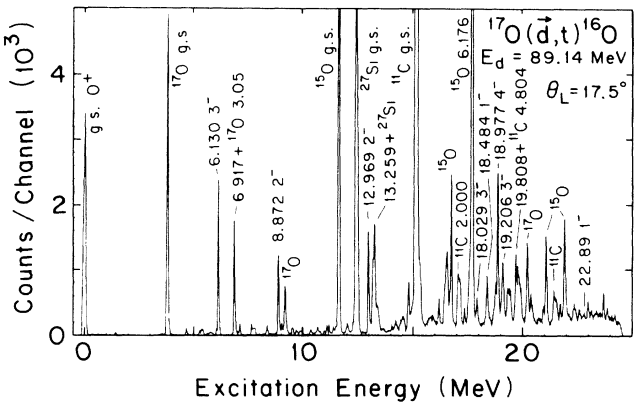

FIG. 1. Spectrum of the $^{17}O(\vec{d},t)^{16}O$ reaction observed at $\theta_{lab}=17.5°$ with a SiO_2 target enriched in ^{17}O. $E_d=89.1$ MeV. Impurity peaks $^{18,16}O(\vec{d},t)^{17,15}O$, $^{28}Si(\vec{d},t)^{27}Si$, and $^{12}C(\vec{d},t)^{11}C$ are indicated.

Improved spectra were obtained by suitably subtracting measured $^{18}O(\vec{d},t)^{17}O$ and $^{16}O(\vec{d},t)^{15}O$ spectra, also taken at $\theta_{lab}=17.5°$, from the spectrum of Fig. 1. First the unwanted $^{18}O(d,t)^{17}O$ spectrum was subtracted out by using data obtained with the SiO_2 target enriched in ^{18}O. (In that process we automatically make a partial subtraction of the ^{15}O and ^{27}Si peaks.) Next the remaining $^{16}O(d,t)^{15}O$ contributions were subtracted by using the data obtained with the natural SiO_2 target. This process left fairly clean spectra for analysis, but still contained most of the (kinematically broadened) $^{28}Si(d,t)^{27}Si$ background.

The spectrum of Fig. 2 was obtained by subtracting enough of the natural SiO_2 data to remove *all* of the ^{27}Si contamination. In this case too much of the $^{16}O(d,t)^{15}O$ spectrum is subtracted. Since the plotting routine did not reproduce negative values, some of the "zeroes" shown in Fig. 2 are actually negative numbers resulting from this unavoidable excess subtraction of ^{15}O peaks. There are very few of these blank spots, and Fig. 2 gives the most

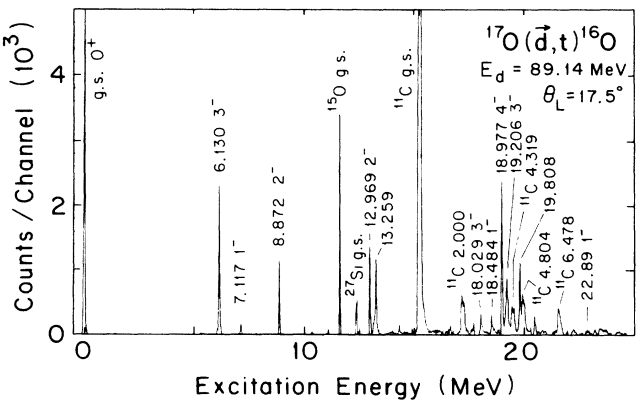

FIG. 2. The $^{17}O(\vec{d},t)^{16}O$ spectrum obtained after subtracting the impurity contributions from the spectrum of Fig. 1 as explained in Sec. III. (Negative values are suppressed.)

informative $^{17}O(\vec{d},t)^{16}O$ spectrum.

The ground state of ^{17}O has spin and parity $J^\pi=\frac{5}{2}^+$, and the shell-model description of ^{17}O is a $1d_{5/2}$ neutron outside a closed ^{16}O core. Pickup of a $1p_{1/2}$ neutron, therefore, will excite the states of ^{16}O with $J^\pi=2^-$ and 3^-, whereas $1p_{3/2}$ pickup will excite $J^\pi=1^-,2^-,3^-$, or 4^- states of ^{16}O. So we expect to see several strong 1^-, 2^-, 3^-, 4^- states along with the strong ^{16}O ground state (with $J^\pi=0^+$). The independent particle (IPM) shell-model predicts one each of the following states: $J^\pi=1^-$, $T=0$; $J^\pi=1^-$, $T=1$; $J^\pi=4^-$, $T=0$, and $J^\pi=4^-$, $T=1$, and two each of the following states: $J^\pi=2^-$, $T=0$; $J^\pi=2^-$, $T=1$; $J^\pi=3^-$, $T=0$ and $J^\pi=3^-$, $T=1$.

Strong peaks were identified by comparison with previous studies[1,6] and the rough spectrograph calibration. The weaker peaks were calibrated by using the known[13] excitation energies of well-known strong peaks. The presence of the ^{11}C peaks facilitated the calibration of the ^{16}O peaks, especially at high excitation. Two weakly excited levels at 20.945 MeV and 22.89 MeV were seen above 20.45 MeV, the last peak identified in previous neutron pickup experiments. The $^{17}O(\vec{d},t)^{16}O$ spectra were analyzed with the computer code AUTOFT.[14] Peak areas were obtained by fitting the spectrum with typical shapes taken from the strong peaks. The error estimates used in the subsequent calculations were the larger of the fitting error or the statistical error. These errors are shown in Figs. 3–8, and 11 and 12, if they exceed the size of the data points.

The cross section and the analyzing power were calcu-

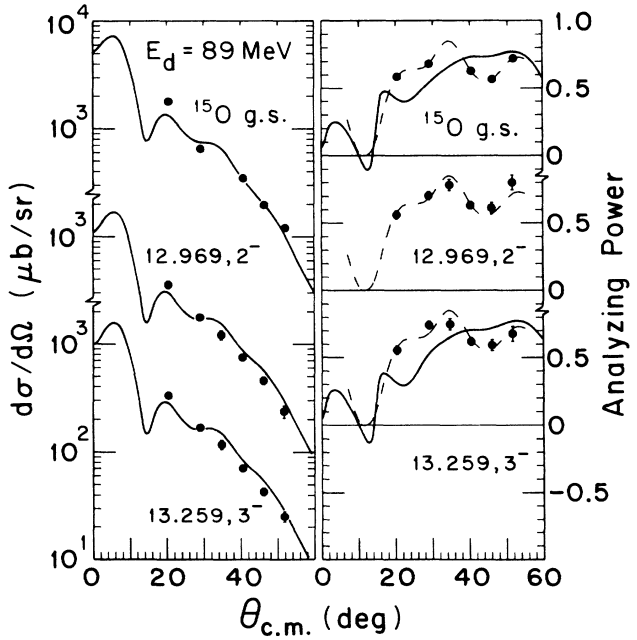

FIG. 3. Angular distributions of cross sections and analyzing powers for states excited by pure $p_{1/2}$ transfer. Solid curves represent DWBA calculations for $p_{1/2}$ neutron pickup. Dashed curves represent empirical templets for $p_{1/2}$. These templets are averages over results of Ref. 3 and present work.

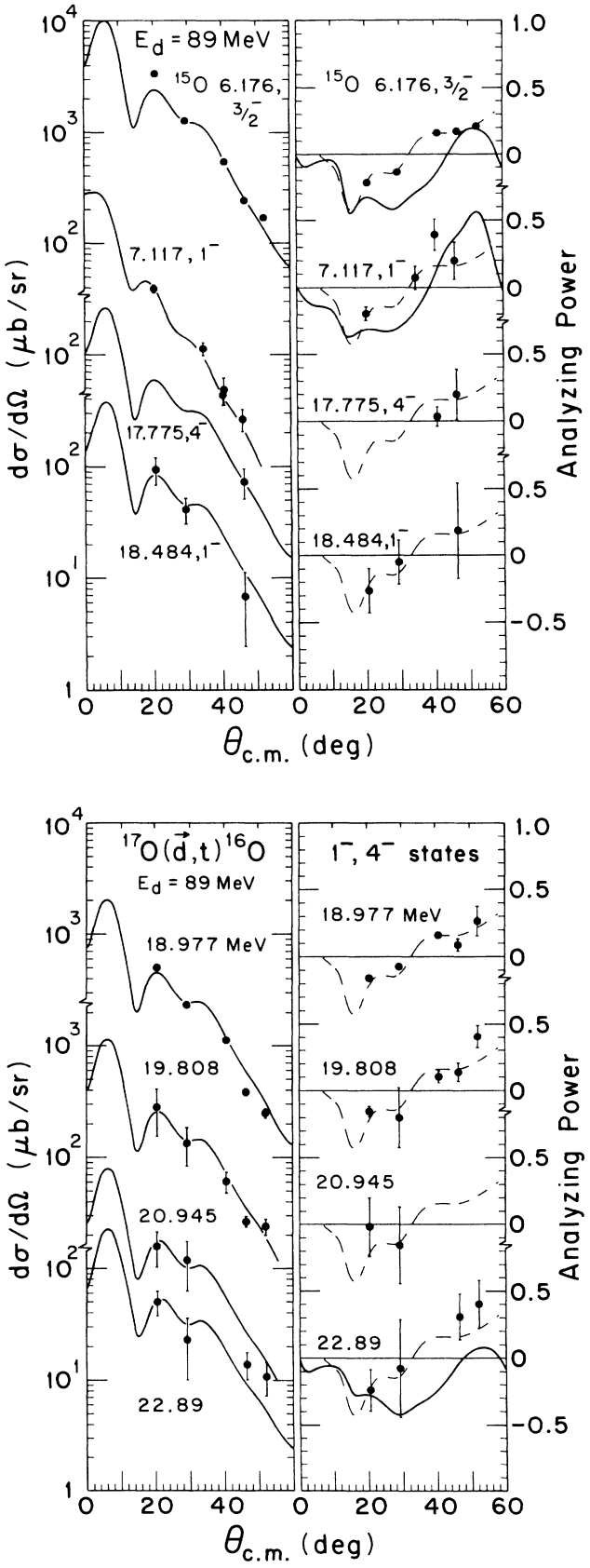

FIG. 4. Angular distributions of cross sections and analyzing powers for the states which are excited by pure $p_{3/2}$ transfer. Solid curves represent DWBA calculations for $p_{3/2}$ neutron pickup. Dashed curves represent empirical templets for $p_{3/2}$.

lated from the relations

$$\frac{d\sigma}{d\Omega}=\frac{P\uparrow(d\sigma/d\Omega)\downarrow+P\downarrow(d\sigma/d\Omega)\uparrow}{P\uparrow+P\downarrow} \quad (1)$$

and

$$A_y=\frac{2}{3}\frac{(d\sigma/d\Omega)\uparrow-(d\sigma/d\Omega)\downarrow}{P\uparrow(d\sigma/d\Omega)\downarrow+P\downarrow(d\sigma/d\Omega)\uparrow} \quad (2)$$

where $P\uparrow$ and $P\downarrow$ are positive numbers and give the vector polarization of the beam.

Out of a total of 32 observed peaks, 19 are 1^-, 2^-, 3^-, or 4^- states. Ten states have been identified as either 0^+, 2^+, 3^+, 4^+, or 5^+ states. 0^+ or 5^+ final-state spins require $d_{5/2}$ neutron pickup, whereas a 4^+ state may be populated by either $d_{5/2}$ or $d_{3/2}$ neutron pickup, and 2^+ or 3^+ final states can be excited by $d_{5/2}$, $d_{3/2}$, or $s_{1/2}$ pickup. All positive parity states [except the ground state (g.s.)] are found to be weak. Weak 0^- states have been identified at 10.957 MeV and 12.796 MeV. In the one-step pickup picture, these two states would have to be excited by $1f_{5/2}$ pickup.

Table I summarizes information from the present experiment. Excitation energies, spins and parities of levels listed in the first three columns of Table I are taken from the compilation of Ref. 13, except for new information

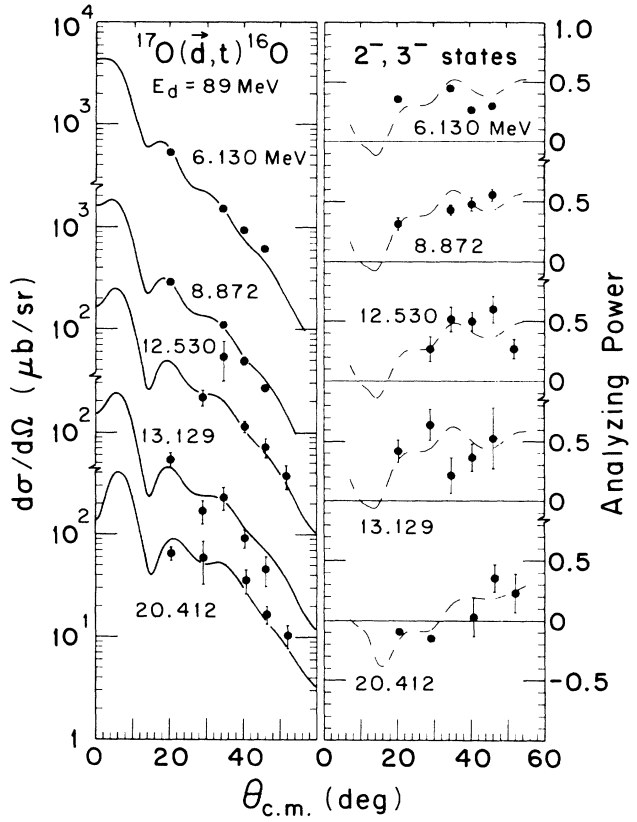

FIG. 5. Angular distributions of cross sections and analyzing powers for $J^\pi=2^-,3^-$ states which can be excited by mixtures of $p_{1/2}$ and $p_{3/2}$ transfer. Solid curves represent DWBA calculations for neutron pickup. Dashed curves represent templet fits. All (solid and dashed) curves include proper mixtures of $p_{1/2}$ and $p_{3/2}$ pickup (see Table IV).

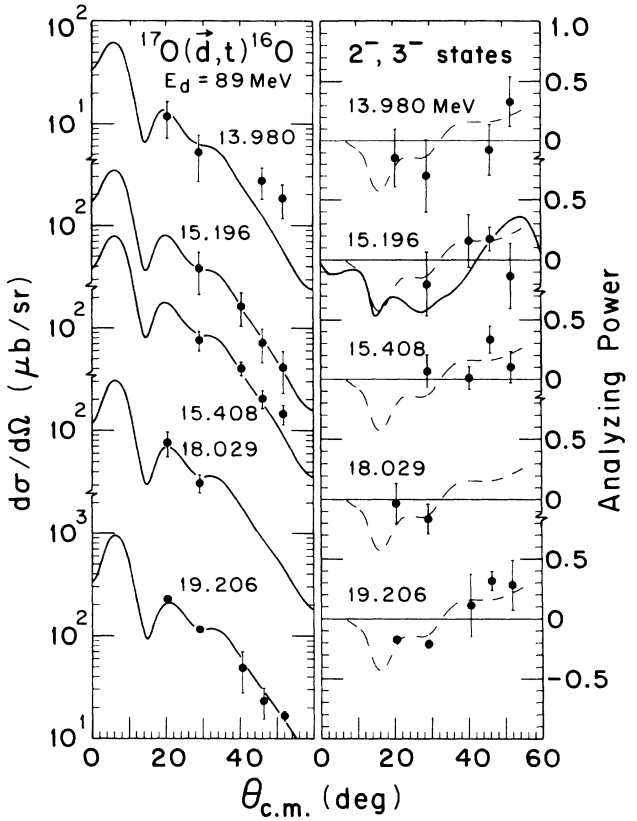

FIG. 6. Angular distributions of cross sections and analyzing powers for $J^\pi=2^-,3^-$ states excited predominantly by $p_{3/2}$ neutron pickup. Solid curves represent DWBA calculations for $p_{3/2}$ neutron pickup. Dashed curves represent experimental templets for $p_{3/2}$. These transitions are best fit by $p_{3/2}$, although, in principle, they may have weak $p_{1/2}$ admixtures.

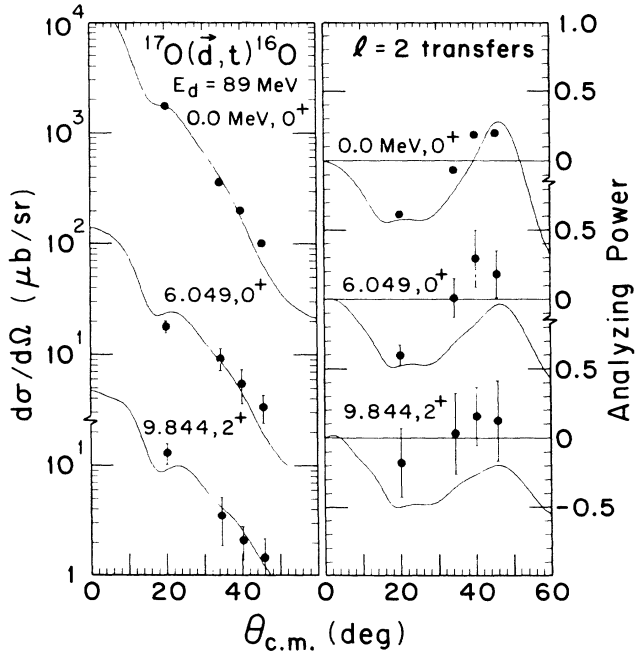

FIG. 7. Angular distributions of cross sections and analyzing powers of positive parity states excited by $1d_{5/2}$ neutron pickup. Solid curves represent DWBA calculations for $1d_{5/2}$ neutron pickup.

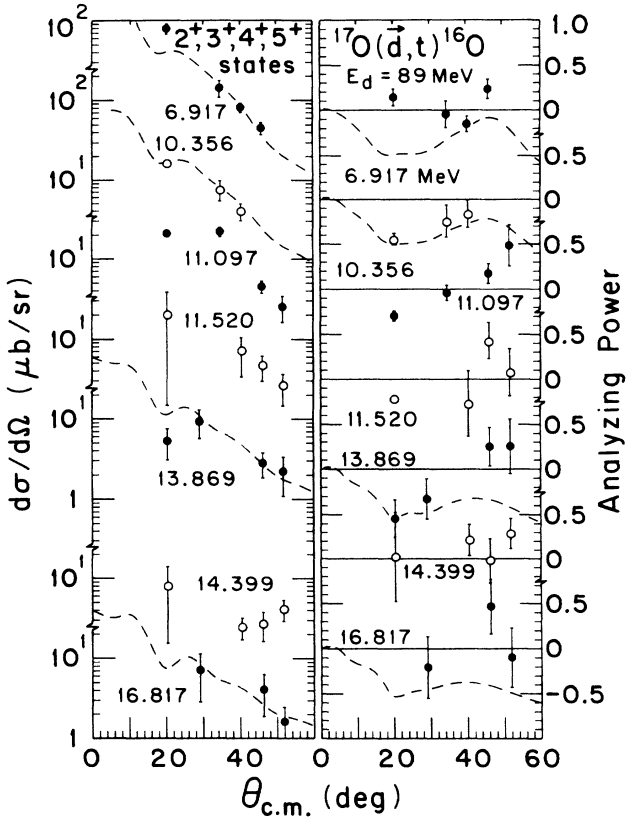

FIG. 8. Angular distributions of cross sections and analyzing powers for weakly excited positive parity states. DWBA calculations for $d_{5/2}$ transfer are shown (dashed curves) for four states which may be excited by $d_{5/2}$ neutron pickup. Other states are probably excited by multistep transfer.

entered for the levels at 13.259, 16.817, and 18.484 MeV, as discussed in Sec. V. Excitation energies deduced in this experiment are listed in column 4. Angular distributions of differential cross sections (σ) and vector analyzing powers (A_y) for the 1^-, 2^-, 3^-, and 4^- final states are shown in Figs. 3–6, whereas those for the positive-parity states are shown in Figs. 7 and 8.

The extraction of absolute cross sections and "absolute" spectroscopic factors depends critically on the knowledge of the thickness of the targets used. The nominal thicknesses of the three targets used in the present experiment were determined by weighing and later reproduced to ±10% in an alpha source measurement. They were cross checked during the experiment by measuring the yields of elastic scattering from the constituent isotopes at $\theta_L = 30°$ with the same apparatus and by comparing them to optical model predictions and to the ^{28}Si(d,d) data of Ref. 15. The latter calibration has the advantage of automatically correcting for target nonuniformity and any insufficiently known solid angles, detector efficiency, or charge integration calibration. Its weakness is the use of secondary standards. Ideally, both normalization methods should agree within their estimated errors, but without *ad hoc* corrections this was not the case for the present measurements. By using optical model predictions for the oxygen isotopes we deduced target thicknesses which are 61%, 68%, and 66%, respectively, of the nominal thicknesses of 2.4, 2.75, and 4.6 mg/cm^2 of the ^{16}O, ^{17}O, and ^{18}O enriched targets. For the natural SiO_2 target, the more direct comparison with the previous ^{28}Si data yields 66% of the nominal thickness.

The 34% difference between the nominal target thick-

TABLE I. Levels populated in ^{17}O($\vec{d},t$)^{16}O.

Prior work[a]			Current results				
E_x (MeV±keV)	J^π	T	E_x (MeV±keV)	l	j	C^2S[c]	$(d\sigma/d\Omega)_{max}$ μb/sr
0.000	0^+	0	0.000	2	$\frac{5}{2}$	1.034±0.084	1736±21.9
6.049±1	0^+	0	6.045±8	2	$\frac{5}{2}$	0.016±0.004	17.9±2.2
6.130	3^-	0	6.131±3	1	$\frac{1}{2}$ $\frac{3}{2}$	0.578±0.137 0.373±0.081	527±21.9
6.917	2^+	0	6.913±4	(2)	$(\frac{5}{2})$	(0.030±0.004)	78.9±11.9
7.117	1^-	0	7.115±3	1	$\frac{3}{2}$	0.055±0.006	39.2±3.2
8.872	2^-	0	8.870±3	1	$\frac{1}{2}$ $\frac{3}{2}$	0.335±0.086 0.137±0.048	289±24.0
9.844	2^+	0	9.841±6	2	$\frac{5}{2}$	0.007±0.003	12.9±2.7
10.356±3	4^+	0	10.354±3	(2)	$(\frac{5}{2})$	(0.016±0.004)	19.9±3.5
10.957±1	0^-	0	10.955±9				6.7±3.4
11.097±2	4^+	0	11.095±6				26.1±5.3
11.520±4	2^+	0	11.525±9				20.0±18.5
12.530±1	2^-	0	12.528±6	1	$\frac{1}{2}$ $\frac{3}{2}$	0.234±0.046 0.036±0.015	53.5±22.3
12.796±4	0^-	1	12.782±23				29.8±5.0

TABLE I. (*Continued*).

Prior work[a]			Current results				
E_x (MeV±keV)	J^π	T	E_x (MeV±keV)	l	j	C^2S[c]	$(d\sigma/d\Omega)_{max}$ μb/sr
12.969	2^-	1	12.971±3	1	$\frac{1}{2}$	0.396±0.101	356±22.2
13.129±10	3^-	0	13.148±14	1	$\frac{1}{2}$ $\frac{3}{2}$	0.058±0.019 0.019±0.012	62.1±17.0
13.259±2	3^-	1[b]	13.256±3	1	$\frac{1}{2}$	0.562±0.106	335±21.9
13.869±20	4^+	0	13.857±30	(2)	$(\frac{5}{2})$	(0.015±0.003)	10.3±4.6
13.980±2	2^-		13.979±17	1	$\frac{3}{2}$	0.016±0.004	11.9±4.7
14.302±3	$4^{(-)}$		14.313±18				24.1±9.2
14.399±2	5^+		14.409±11				7.8±6.2
15.196±3	2^-	0	15.195±32	1	$\frac{3}{2}$	0.106±0.030	38.4±16.8
15.408±2	3^-	0	15.414±6	1	$\frac{3}{2}$	0.242±0.038	76.3±16.7
16.817±2	3^+	1	16.808±11	(2)	$(\frac{5}{2})$	(0.015±0.005)	72.±4.3
17.775±11	4^-	0	17.776±11	1	$\frac{3}{2}$	0.089±0.045	48.3±13.2
18.029±5	$3^{(-)}$	1	18.027±7	1	$\frac{3}{2}$	0.102±0.023	76.1±20.8
18.484±6	1^-	1	18.483±17	1	$\frac{3}{2}$	0.129±0.028	94.6±26.0
18.977±6	4^-	1	18.978±7	1	$\frac{3}{2}$	0.706±0.065	502±11.2
19.206±12	3^-	1	19.210±14	1	$\frac{3}{2}$	0.338±0.036	227±9.9
19.808±11	4^-	0	19.806±11	1	$\frac{3}{2}$	0.423±0.116	281±127
20.412±17	2^-	1	20.481±8	1	$\frac{1}{2}$ $\frac{3}{2}$	0.015±0.018 0.144±0.029	65.3±10.0
20.945±20	1^-	1	20.922±30	1	$\frac{3}{2}$	0.032±0.009	15.6±5.6
22.89±10	1^-	1	22.857±60	1	$\frac{3}{2}$	0.109±0.023	50.0±12.4

[a]Reference 13.
[b]Reference 6 (see Sec. V).
[c]Errors shown include statistics and fitting error (see Sec. IV). Note that errors from $p_{1/2}$-$p_{3/2}$ decomposition are correlated.

ness and the thickness deduced from elastic scattering is more than twice the uncertainty expected and suggests a scale error in one of the absolute cross-section determinations. For the reasons indicated above we prefer (and use) the absolute normalization based on deuteron elastic scattering. We assign it an error of 20%; however, the lack of a plausible explanation for the disagreement raises concerns about the reliability of this error estimate.

IV. DWBA CALCULATIONS AND EMPIRICAL UNFOLDING OF j TRANSFERS

A. Reaction calculations and spectroscopic factors

Finite-range distorted-wave Born approximation (DWBA) calculations have been carried out with the code FRUCK2.[16] In this code the wave function of the bound neutron is generated with a Woods-Saxon potential. We employed the surface peak method to compute the neutron form factor. This improved way to describe the bound neutron was suggested by Austern and Rae[17] and can have effects of order 20%. However, for this study the comparison with the conventional separation energy method shows differences in computed cross sections of only about 1%.

The deuteron optical-model parameters for the entrance channel were taken from the global parameters of Daehnick, Childs, and Vrcelj.[15] As triton elastic-scattering data do not exist in the energy region of interest, we used the optical-model potentials for $^{16}O(^3He,^3He)$ at 79 MeV (Ref. 18) for the exit channel (see Table II). Of the two different sets of parameters that fit the ^3He elastic scattering data well, we used the deeper potential. The well radius (r_0) and diffuseness (a_0) parameters used for the form factor potential were 1.28 and 0.85 fm, respectively.[3] The spin-orbit parameter

TABLE II. Optical-model potential parameters used in DWBA calculations.

	V	r_0	a_0	W_S	W_D	r_I	a_I	V_{LS}	r_{LS}	a_{LS}	r_C	Ref.
d	68.061	1.17	0.860	7.959	6.558	1.325	0.679	4.745	1.07	0.66	1.3	15
t	205.0	1.08	0.72		14.9	1.35	0.67	11.34	0.73	0.67	1.3	18

λ was kept fixed at 20 and the conventional nonlocality parameters $\beta_d=0.54$ and $\beta_t=0.25$ were employed for the scattered waves.

We find reasonably good agreement between the DWBA predictions and the experimental results for the differential cross sections, but consistent with the ^{14}N results[3] analyzing power predictions agree with the data only qualitatively. Spectroscopic strengths G were extracted by comparing the experiment cross section with the predictions of FRUCK2, using the relation

$$\left[\frac{d\sigma}{d\Omega}\right]_{\text{pickup}} = gG\left[\frac{d\sigma}{d\Omega}\right]_{\text{FRUCK2}}, \tag{3}$$

where $(d\sigma/d\Omega)_{\text{pickup}}$ and $(d\sigma/d\Omega)_{\text{FRUCK2}}$ are the experimental and the predicted cross sections, respectively; g is the light particle spectroscopic strength,[19] which for this reaction is $\frac{3}{2}$. For pickup G is equal to C^2S, where C is an isospin Clebsh-Gordan coefficient and S is the spectroscopic factor.

DWBA fits to cross sections in our previous work,[3] which were measured over the wider angular range, show that for $l=1$ calculations normalized to the first stripping peak, DWBA curves stay systematically above the data for angles above 20°. Hence we infer that for the fits of Figs. 3–7 the deduced spectroscopic strengths for the $l=1$ transitions are lower than the "best" values, and therefore, should be renormalized. By using Ref. 3 we calculate this renormalization factor to be 1.35 ± 0.25 and 1.10 ± 0.10, respectively, for $p_{1/2}$ and $p_{3/2}$ transfers. On the other hand, for the $l=2$ transitions we find that the deduced spectroscopic strengths would be higher if σ_{DWBA} were normalized to the stripping peak, and therefore, should be renormalized by a factor of 0.94 ± 0.06. The ^{17}O$(d,t)^{16}$O spectroscopic strengths reported in Table I and used in subsequent calculations include this correction. With these assumptions and normalizations we deduce $\Sigma C^2S(p_{1/2})=2.18\pm0.42$ and $\Sigma C^2S(p_{3/2})=3.06\pm0.32$. Hence the total deduced $l=1$ spectroscopic strength is $87\pm12\%$ of the conventional sum rule. These errors include all uncertainties from statistics and relative normalizations but not, of course, the significant uncertainty inherent in the DWBA model. For essentially the same levels Mairle *et al.*[6] had found 88% of the $l=1$ strength in the ^{17}O$(d,t)^{16}$O experiment at $E_d=52$ MeV. We note that the results are quite sensitive to the chosen form factor well. Spectroscopic strengths computed with well parameters typical[20] for heavier nuclei ($r_0=1.20$ and $a_0=0.75$ fm) exceeded the shell-model limit by 10%.

In view of our intent to deduce effective matrix elements (Sec. VI), it is important to cross-check the spectroscopic factors extracted here for possible scale errors. It is known that the form factor geometry for light targets must be larger than the (1.25; 0.65) or equivalent convention used for heavy nuclei. The geometry $r_0=1.28$ and $a_0=0.85$ fm agrees with expectation, but a generally accepted prescription does not exist. One useful test is to evaluate the spectroscopic strengths of the simultaneously observed $1/2^-$ ground state and the strongly excited $3/2^-$ level at 6.176 MeV of ^{15}O. Since the ground state of ^{16}O has $J^\pi=0^+$, these states must be excited by neutron pickup of $p_{1/2}$ and $p_{3/2}$, respectively. Table III gives the results and comparison with other work. In that table the two sets of values from Ref. 21 were obtained by using two different sets of parameters for tritons in a (d,t) experiment at $E_d=29$ MeV. The results in Ref. 22 were obtained in a (p,d) experiment at $E_p=65$ MeV. The last column of Table III shows the results of a weak coupling model calculation by Ellis-Engeland.[23] We note that the choice of $r_0=1.28$ and $a_0=0.85$ gives very good agreement with other experiments, but a 25% higher value than the ^{15}O calculation.

A valuable test of the completeness of the observed strength is possible by analyzing the distribution of spectroscopic factors shown in Fig. 13. A very weak $p_{1/2}$ transfer is observed as high as 20.4 MeV, but clearly the bulk of the $p_{1/2}$ strength is found in a 9-MeV interval below 14 MeV. Hence the probability that states with significant $p_{1/2}$ strength could be found above 25 MeV is very small. On the other hand, the observed $p_{3/2}$ strength is largest near 18 MeV and is spread over at least 20 MeV. It is likely that about 15% of the $p_{3/2}$ strength remains unobserved and lies above 25 MeV. We infer that the spectroscopic factors of Fig. 13 and Table I have reasonable error estimates, but may be systematically high by about 10%.

B. Empirical unfolding of $p_{1/2}$-$p_{3/2}$ mixing

In order to estimate the contribution of each j transfer to 2^- and 3^- states where mixed j transfer is possible, we make use of the fact that the vector analyzing power (A_y) shows a strong and regular j dependence. This is evident from Figs. 3 and 4, which include the A_y for the strong transitions to the ^{15}O g.s. and the 6.176-MeV state. As noted above, these two states must be excited by pure $p_{1/2}$ and $p_{3/2}$ transfers, respectively.

The A_y decomposition was done by constructing two "standard" curves, one for $p_{3/2}$ transfers and the other for $p_{1/2}$ transfers, which serve as templets for pure j transitions. Figure 9 shows A_y values for the 7.117, 18.977, and 19.808 states of ^{16}O and for the ^{15}O (6.176 MeV)

TABLE III. Comparison of C^2S for ^{15}O *gs* and 6.176-MeV state with previous works (form factor geometries shown in parentheses).

E_x (MeV)	C^2S using[a] (1.28, 0.85)	C^2S using[a] (1.20, 0.75)	Ref. 21 (1.25, 0.65)	Ref. 21 (1.25, 0.65)	Ref. 22 (1.25, 0.65)	Ref. 23
0.000	2.23±0.46	2.83±0.56	2.50	2.25	2.4	1.51
6.176	3.30±0.34	4.18±0.40	3.34	3.28	3.4	2.90

[a]Errors shown include statistics and fitting error (see Sec. IV).

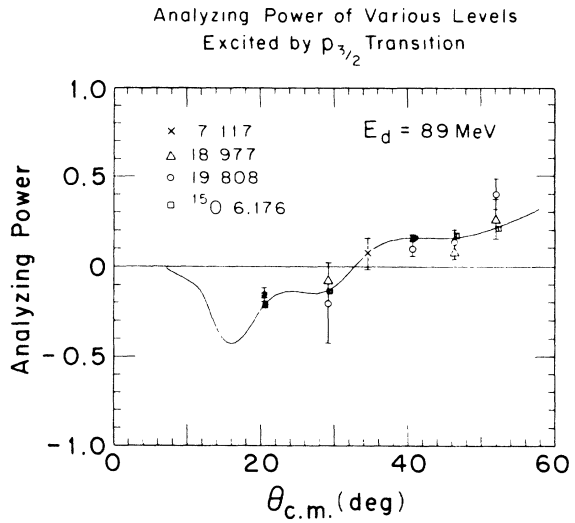

FIG. 9. Comparison of measured $p_{3/2}$ analyzing powers of transitions to various 1^- and 4^- states of ^{16}O and the $3/2^-$(6.176 MeV) state of ^{15}O with a deduced "standard" shape ($p_{3/2}$ templet) for the analyzing powers for pure $p_{3/2}$ transfers. The solid curve represents a fit to these points and to small angle $^{15}N(\vec{d},t)^{14}N$ data.

state, which must be excited by pure $p_{3/2}$ transfers. The "standard" shape (solid curve) was obtained by taking a weighted average of these data and the forward angle data for $^{15}N(\vec{d},t)^{14}N$. To account for the moderate Q value and mass differences for these transitions, we assign an additional estimated error of ± 0.025 to the averaged value of A_y. A_y of the ^{15}O g.s. is taken as the "standard" shape for pure $p_{1/2}$ transfer and is shown in Fig. 10. The extraction of different j contributions was done by performing least square fits of these templets to the data.

In general, such unfolding must use transition amplitudes rather than their corresponding cross sections. In the present case, DWBA predictions are too rough to be used for a detailed A_y analysis. However, they should be good enough to estimate the importance of cross terms that are ignored if the unfolding is based on cross sections. We used DWBA to compare A_y calculations for $p_{1/2}$ and $p_{3/2}$ mixing by coherent or incoherent addition of transition amplitudes. The differences were small and did not exceed the errors assigned to our templet shapes.

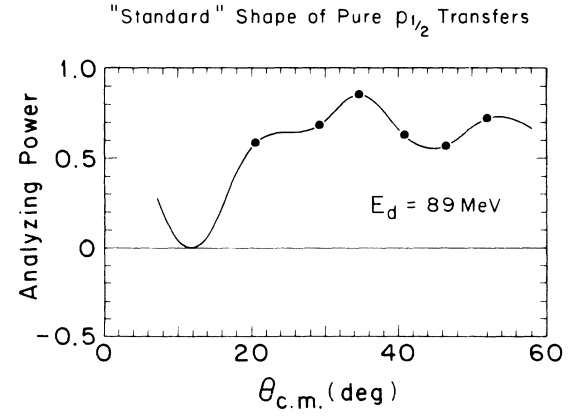

FIG. 10. "Standard" shape for the analyzing powers for pure $p_{1/2}$ pickup obtained from the transition to the $J^\pi = \frac{1}{2}^-$ ^{15}O ground state. (Selection rules require pure $p_{1/2}$ transfer to this state.) The solid curve represents a fit to these points and to small angle $^{15}N(\vec{d},t)^{14}N$ data.

V. DISCUSSION OF INDIVIDUAL LEVELS

The angular distributions $\sigma(\theta)$ for the negative parity states of ^{16}O shown in Figs. 3–6, show the characteristic shape for $l=1$ neutron pickup. Owing to the unavailability of ^{16}O data at smaller angles it is not possible to distinguish different j transfers from the shape of $\sigma(\theta)$. However, the shapes of $A_y(\theta)$ for $p_{3/2}$ and $p_{1/2}$ transfers are strikingly different as is apparent from Figs. 9 and 10. Figure 3 shows the levels excited by pure $p_{1/2}$ neutron pickup, whereas the levels shown in Fig. 4 are excited by pure $p_{3/2}$ neutron pickup. Consistent with the results of $^{15}N(\vec{d},t)^{14}N$ experiment[3] we find that for $p_{1/2}$ pickup A_y remains positive for the entire range of observation ($\theta_{c.m.} \sim 20°$–$50°$), whereas for $p_{3/2}$ pickup A_y is negative for smaller angles and then becomes positive between 30° and 40°. The DWBA predictions agree qualitatively.

The J^π and T values used in Table I are taken from a compilation,[13] except for the levels at 13.259, at 16.817, and at 18.484 MeV. For the 13.259-MeV level we entered $T=1$, following the identification by Mairle *et al.*[6] of its parent state in ^{16}N at $E_x=0.297$ MeV. We take $J^\pi=3^+$, $T=1$ for the 16.817-MeV state following the work of Refs. 24 and 25. Finally, we have set $J^\pi=1^-$ for the level at 18.484 MeV following the phase-shift analysis of the $^{15}N(\vec{p},p_0)^{15}N$ data by Darden *et al.*[24] The $T=1$ assignment comes again from the work of Mairle *et al.*, who found its parent state in ^{16}N at 5.74 MeV.

For all negative-parity states above 13.259 MeV, the observed analyzing power is consistent with pure $p_{3/2}$ pickup, except for the level at 20.412 MeV which seems to show a weak $p_{1/2}$ component. A_y for the levels at 12.969 MeV and 13.259 MeV shows complete agreement with the standard $p_{1/2}$ shape indicating that they are excited by nearly pure $p_{1/2}$ neutron transfer (see Fig. 3). Extraction of configuration mixing for ^{16}O by utilizing the shapes of A_y has been attempted previously[1,8] for $(^3He,\alpha)$ and $(\vec{d},t)$ reactions. Table IV summarizes the results. A major difference between the present results and previous work is that we see evidence of strong mixing of $p_{1/2}$ and $p_{3/2}$ transitions to the 6.130-MeV state, whereas formerly this has been *assumed* to be a pure $p_{1/2}$ transition. If we drop this assumption and reanalyze the data of Ref. 1, using their typical shapes for pure $p_{1/2}$ and $p_{3/2}$ transfers, the mixing deduced agrees with our results. A second major difference is seen for the 8.872-MeV level. We see appreciable configuration mixing for this level as well, whereas in Ref. 1 it is stated that this level is excited by pure $p_{1/2}$ transfer. In Ref. 8 it was concluded that "there is a weak $p_{3/2}$ component" in this transition.

The templet fits show fairly large χ^2 values for the two states with strong mixing. As a check an alternate

TABLE IV. Comparison of $p_{1/2}$-$p_{3/2}$ mixing with other work.

	Present work			Ref. 1	Ref. 8
E_x (MeV)	J^π, T	nl_j	% mixing[a]	% mixing	% mixing
6.130	$3^-,0$	$1p_{1/2}$	56.6±8.4	67.3±11[b]	100.0
		$1p_{3/2}$	43.4∓8.4	32.7∓11	0.0
8.872	$2^-,0$	$1p_{1/2}$	66.3±11.3	67.5±13[b]	Dominant
		$1p_{3/2}$	33.7∓11.3	32.5∓13	Weak
12.530	$2^-,0$	$1p_{1/2}$	51.3±17.8		
		$1p_{3/2}$	48.7∓17.8		
12.969	2^-1	$1p_{1/2}$	100.0	100.0	
		$1p_{3/2}$	0.0	0.0	
13.129	3^-0	$1p_{1/2}$	70.6±19.2		
		$1p_{3/2}$	29.4∓19.2		
13.259	$3^-,1$	$1p_{1/2}$	100.0	100.0	
		$1p_{3/2}$	0.0	0.0	
15.196	$2^-,0$	$1p_{1/2}$	0.0	~25	
		$1p_{3/2}$	100.0	~75	
15.408	$3^-,0$	$1p_{1/2}$	0.0	~25	
		$1p_{3/2}$	100.0	~75	
20.412	$2^-,1$	$1p_{1/2}$	6.8±8.0	0.0	
		$1p_{3/2}$	93.2∓8.0	100.0	

[a]Errors shown include statistics and fitting error. Note that errors from $p_{1/2}$-$p_{3/2}$ decomposition are correlated.
[b]These ratios are obtained after reanalyzing the published data. See Sec. IV.

decomposition of these two transitions was made with the $p_{3/2}$ and $p_{1/2}$ templets from our previous work.[3] The mixing extracted was in full agreement with that from the $^{17}O(\vec{d},t)^{16}O$ templets. Figure 11 compares pure and mixed $A_y(\theta)$ curves with the data for these states. It is apparent that the curve corresponding to the minimum value of χ^2 does not fit the data for the 6.130-MeV (3^-) level overly well. In reanalyzing the data from Ref. 1 for this level we drew a similar conclusion. This may signal an appreciable two-step contribution for this transition, and if so, the mixing ratio deduced may have an uncertainty larger than that deduced from statistics.

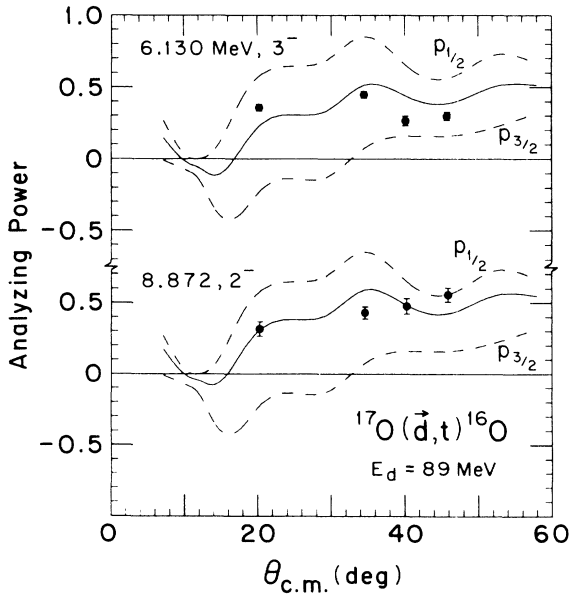

FIG. 11. Analyzing powers of transitions leading to the 6.130- and 8.872-MeV states of ^{16}O. The solid curves represent mixtures of the standard A_y templets (dashed curves) that best fit the data. Both states show unexpectedly strong mixing of $p_{1/2}$ and $p_{3/2}$ transfer.

Several shell model calculations for ^{16}O are available (Refs. 9 and 10, 26–29). The calculations of Refs. 9 and 26 do not include the $1p_{3/2}$ and $1d_{3/2}$ shells, while the rest do include them. From Table 5 of Ref. 6 we see that the small amounts of $p_{1/2}$-$p_{3/2}$ mixing for the $T=0$ MeV states at 6.130 MeV (3^-) and at 8.872 MeV (2^-) predicted by the RPA calculations of Ref. 27 and the Tamm-Dancoff calculations of Ref. 28 are not consistent with our experimental results. Both of these calculations predict very dominant $p_{1/2}$ transitions for these two states.

Two 0^- states observed at 10.957 MeV and 12.796 MeV could be excited only by $f_{5/2}$ neutron pickup in a one-step process. But comparisons of the data with $f_{5/2}$ calculations of $\sigma(\theta)$ and $A_y(\theta)$ show no signature of $l=3$. The absence of forward angle data and large statistical errors for these two states prevent drawing firm conclusions.

Isospin mixing between the 2^- states at 12.530 and at 12.969 MeV has been pointed out by several authors.[30,31] The intensity ratio of the two 2^- and 3^- $T=1$ states at 12.969 and at 13.259 MeV and that of parent states in ^{16}N, the 2^- ground state and the 3^- 0.297-MeV state, differ by about 50%, consistent with the result by Wagner *et al.*[30] The spectroscopic strengths for the ^{16}N states have been taken from Ref. 6. The ratio of the spec-

troscopic strengths of the above-mentioned two states in ^{16}O is 1.05, compared to the ratio of 0.70 for the corresponding parent states in ^{16}N. The excess spectroscopic strength $C^2S=0.195$ of the 12.969-MeV level of ^{16}O over that of its parent ground state in ^{16}N is a result of strong isospin mixing. Following the arguments of Ref. 30 we consider this excess to come from the 12.530-MeV state as shown in Table V.

The level observed at 14.302 has been assigned $J^\pi=4^{(-)}$ in the literature. In the present experiment a 4^- state should be excited only by $p_{3/2}$ neutron pickup. From Fig. 12 we see that the A_y does not resemble the standard shape of a pure $p_{3/2}$ transfer. Consequently we suspect that it is not a 4^- state.

The state observed at 17.778 MeV was masked by the 6.178-MeV state of ^{15}O at forward angles. A ^{27}Si peak and the strong ^{11}C g.s. and 2.000 MeV peaks interfered with this peak at all angles. We associate a 50% arrow with the C^2S value extracted for the 17.778-MeV state.

We see nine positive-parity states in addition to the strong ^{16}O ground state. The positive-parity transitions, other than the ^{16}O ground state transition, are shell model "forbidden" and very weak, in (qualitative) agreement with Ref. 9. Their spectroscopic factors indicate very weak s-d shell admixtures in the ground state of ^{16}O [with an observed strength of $\Sigma C^2S(d5/2)=0.10$]. Hence our measurement disagrees with the results of Glaudemans[10] who calculated s-d shell admixtures of about 20%.

We obtain $C^2S=1.03\pm0.08$ for the ground state, in agreement with a simple independent particle model (IPM). Values of 0.74 ± 0.11 and of 0.47 were found in Refs. 6 and 1, respectively. The shape of A_y for the transition to the ground state is consistent with the shape of A_y for $d_{5/2}$ transfer.[3] From the A_y curves for the positive-parity states we infer that the states at 6.049 and at 9.844 MeV are also excited by $d_{5/2}$ transfer, with C^2S values of 0.02 and 0.01, respectively. The states at 6.917, 10.356, 13.869, and 16.817 MeV are probably also excited by $d_{5/2}$ transfer. The partial sum of the C^2S for these four (doubtful) states is 0.08. Three other positive-parity states are probably excited by multistep processes.

Summing $p_{1/2}$ transitions we find $\Sigma C^2S(p_{1/2};2^-)=0.98\pm0.19$ and $\Sigma C^2S(p_{1/2};3^-)=1.20\pm0.24$, com-

TABLE V. $^{17}O(d,t)^{16}O$ spectroscopic factors compared with other work.

l_j	J^π	T	E_x (MeV)	C^2S (present) $^{17}O(d,t)\pm$ error	C^2S (Ref. 6) (d,t)	C^2S (Ref. 1) $(^3He,\alpha)$	Shell-model partial sums
$p_{1/2}$	2^-	0	8.872	0.335±0.086	0.33	0.20	
		0	12.530	(0.039+0.195[a])±0.046	0.19[a]		0.42
		0	15.196	<0.03		0.13	
		1	12.969	(0.591-0.195[a])±0.101	0.69-0.19[a]	0.96	0.42
		1	20.481[b]	0.015±0.018			
	3^-	0	6.130	0.578±0.137	0.46	0.49	
		0	13.129	0.058±0.019			0.58
		0	15.408	<0.02		0.13	
		1	13.259	0.562±0.106	0.70	0.96	0.58
		0	7.117	0.055±0.006	0.04		0.25
$p_{3/2}$	1^-	1	18.484	0.129±0.028	0.25	0.24	
		1	20.945	0.032±0.009			0.25
		1	22.89	0.109±0.023			
	2^-	0	8.872	0.137±0.048			
		0	12.530	0.036±0.015	0.07		
		?	13.980	0.016±0.004			0.42
		0	15.196	0.106±0.030	0.12	0.39	
		1	20.481[b]	0.144±0.029	0.12	0.21	0.42
	3^-	0	6.130	0.373±0.081			
		0	13.129	0.019±0.012			0.58
		0	15.408	0.242±0.038	0.37	0.39	
		1	18.029	0.102±0.023	0.12		0.58
		1	19.206	0.338±0.036	0.50	0.87	
	4^-	0	17.775	0.089±0.045	0.17	0.31	0.75
		0	19.808	0.423±0.116	0.52	0.35	
		1	18.977	0.706±0.065	0.73	0.87	0.75
Sums:	$\Sigma C^2S=$ $l=1$			5.234	5.19	6.50	6.0

[a]Isospin correction (see Sec. V).

[b]Energies are from Ref. 13 except for this new level. Note that errors from $p_{1/2}$-$p_{3/2}$ decomposition are correlated.

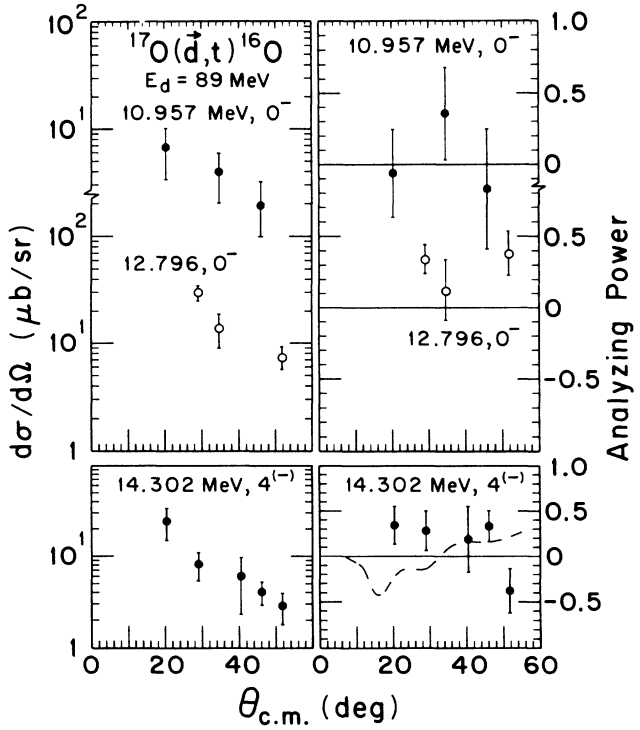

FIG. 12. Angular distributions of cross sections and analyzing powers for two 0^- states and a $4^{(-)}$ state weakly excited in this reaction. These states are probably excited by multistep transfer.

pared to shell model sums of 0.84 and 1.16, respectively. For $p_{3/2}$ transitions the strength found in this experiment is 76% of the shell-model sum rule, the partial sums for $J^\pi = 1^-$, 2^-, 3^-, and 4^- states being 0.32 ± 0.04, 0.44 ± 0.06, 1.07 ± 0.13, and 1.22 ± 0.16, compared to shell model values of 0.50, 0.84, 1.16, and 1.5, respectively. These numbers are consistent with the distribution of $p_{3/2}$ strength shown in Fig. 13, which would suggest that some of it has remained unobserved, and probably lies above 25 MeV.

VI. EFFECTIVE INTERACTIONS

Given the spin assignments and spectroscopic strengths in Table V we can compute residual-interaction matrix elements of the $(1p_{1/2}^{-1}1d_{5/2})$ and $(1p_{3/2}^{-1}1d_{5/2})$ configurations for each allowed combination of T and J^π values. We determine the energy centroid of a particular configuration of each J^π and T by weighting each energy level with its spectroscopic strength. Then we subtract the unperturbed multiplet energy for that particular configuration from this centroid energy to obtain the above-mentioned matrix elements. The unperturbed multiplet energy for the $(p_{1/2}^{-1}d_{5/2})$ configuration is given by

$$E_0(p_{1/2}^{-1}) = B(^{17}\mathrm{O}) + B(^{15}\mathrm{O}) - 2B(^{16}\mathrm{O}) ,$$

where B stands for binding energy (mass excess in MeV) of a particular nucleus. For the $(p_{3/2}^{-1}d_{5/2})$ configuration $E_0(p_{3/2}^{-1})$ is given by

$$E_0(p_{3/2}^{-1}) = B(^{17}\mathrm{O}) + B(^{15}\mathrm{O}^*) - 2B(^{16}\mathrm{O}) ,$$

where the asterisk denotes that the nucleus listed is excited to its single-particle (j) level. We obtain $E_0(p_{1/2}^{-1}) = 11.526$ MeV and $E_0(p_{3/2}^{-1}) = 17.702$ MeV.

Table VI shows the new centroid energies $\mathcal{E}_{\mathrm{cent}}$ and the particle-hole matrix elements $E(J)$ obtained in this study. These results are compared with the summary of Ref. 4.

Because of the likelihood of undetected strength, particularly for $p_{3/2}$, the centroid values $\mathcal{E}_{\mathrm{cent}}$ derived correspond to lower limits for the true values. Accordingly, the deduced matrix elements which correspond to these centroid values also represent the lower limits for matrix elements $E(J)$. To estimate the effect of undetected high-lying components we estimate the missing strength (by using partial shell model sum rules) and allocate it to 23.0 MeV. The matrix elements derived in this way are

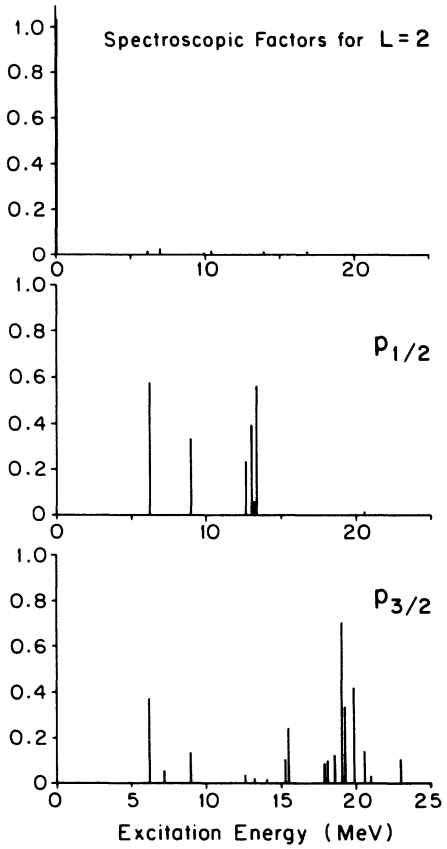

FIG. 13. Distribution of spectroscopic factors C^2S with excitation energy. The data are ordered by j transfer. Note the very small $d_{5/2}$ spectroscopic factors for all states but the ground state which would make them difficult to detect above 20 MeV.

TABLE VI. Matrix elements $E(J)$ for particle-hole residual interactions compared with previous work.

Configuration	J^π	T	$\mathcal{E}_{cent}$[a]	$E(J)$[b] ^{16}O, new	$E(J)$ from Ref. 4 from ^{16}O	from ^{16}N
$p_{1/2}^{-1}d_{5/2}$	2^-	0	10.976	-0.55 ± 0.6	-1.10 ± 0.3	
		1	13.313	1.79 ± 0.1	1.45	1.585 ± 0.1
	3^-	0	7.368	-4.16 ± 0.6	-3.94 ± 1.45	
		1	13.435	1.91 ± 0.2	1.74	1.88 ± 0.1
$p_{3/2}^{-1}d_{5/2}$	1^-	0	13.311	-4.39 ± 6.2	-1.35 ± 6.0	
		1	21.154	3.45 ± 0.6	4.74 ± 2.0	4.81 ± 1.40
	2^-	0	13.496	-4.21 ± 1.6	-4.325 ± 1.0	
		1	21.305	3.60 ± 0.8	1.56 ± 0.2	1.82 ± 0.1
	3^-	0	10.536	-7.17 ± 1.4	-1.11 ± 1.3	
		1	19.432	1.73 ± 0.5	1.30 ± 0.1	1.46
	4^-	0	20.017	2.31 ± 0.6	1.865 ± 0.25	
		1	19.095	1.39 ± 0.1	1.24 ± 0.1	$1.7(\pm0.2)$

[a]Energy centroids of levels for a given configuration $|j_1 j_2\rangle J^\pi, T$.
[b]Our best estimates of the matrix elements (see Sec. VI). Unperturbed multiplet energies used are $E_0(p_{1/2}^{-1})=11.526$ MeV, $E_0(p_{3/2}^{-1})=17.702$ MeV.

our upper estimates $E(J)_{max}$ of the true values. (23.0 MeV was chosen, because we could not resolve any peaks above this energy and there are no known $l=1$ peaks beyond 22.89 MeV.) The $E(J)$ ranges shown in Table VI are chosen in such a way that they include both $E(J)_{min}$ and $E(J)_{max}$. The choice of 23.0 MeV as the centroid of the missing strength is somewhat arbitrary and therefore this assigned range is tentative. For terms where the spectroscopic sums meet or exceed the sum rule limits, we compute an overall uncertainty based on the reliability of the cross sections and the templet fit, where appropriate. The "best" value for $E(J)$ is then chosen in such a way that the $E(J)$ range brackets the lower and the upper estimates. It is clear that the missing strength and hence estimated uncertainties in $E(J)$ are subject to the uncertainties of the absolute cross sections as well as to ambiguities of the DWBA model. The errors given for $E(J)$ merely indicate a relative measure of the reliability of the data. The same comment is applicable to the matrix elements obtained in Ref. 4.

We find that $(p_{1/2}^{-1}d_{5/2})$ matrix elements agree well with Ref. 4, especially with the better known $T=1$ values deduced from ^{16}N. For the $(p_{3/2}^{-1}d_{5/2})$ matrix elements there are six agreements, but two significant differences for the configurations with $J^\pi=2^-$, $T=1$, and for $J^\pi=3^-$, $T=0$. The latter is large and can be traced to assigning a $p_{3/2}^{-1}d_{5/2}$ component to the 6.130-MeV(3^-) state which is almost as large as the $p_{1/2}^{-1}d_{5/2}$ component. Also, it is to be noted that in Ref. 4 the 18.484-MeV level was taken as $J^\pi=2^-$, whereas we assume $J^\pi=1^-$, as has been discussed in Sec. V. Clearly, the postulated $p_{3/2}^{-1}$ admixtures to the low-lying states have a large effect and should be independently verified. In addition, the continuing shortfall of observed $p_{3/2}$ strength (24%) makes the $(p_{3/2}^{-1}d_{5/2})$ matrix elements subject to correction in the future.

VII. SUMMARY AND CONCLUSIONS

In summary, we searched for $l=1$ transitions up to 25 MeV in excitation energy, and saw essentially all of the $p_{1/2}$ strength. About 25% of the $p_{3/2}$ strength is still unobserved and must be expected near and above 25 MeV. Only a small fraction (0.1) of the "missing" strength was found in $l=2$ pickup. Above the 20.45-MeV peak, two new $1^-, T=1$ peaks, at 20.945 and 22.89 MeV, have been identified in our search for missing $J^\pi=1^-$ strength. On the other hand, we did not find any new $J^\pi=1^-$, $T=0$ state. No measurable $l=3$ strength was found in the entire spectrum.

Experimental discrimination between $p_{1/2}$ and $p_{3/2}$ transfers was found to be excellent. By constructing standard $p_{1/2}$ and $p_{3/2}$ A_y templets from pure transitions we could unfold constituent j contributions for the 2^- and 3^- states. This study suggests significantly more mixing between different j transfers than predicted theoretically,[27,28] particularly for the two $T=0$ states at 6.130 ($J^\pi=3^-$) and 8.872 MeV ($J^\pi=2^-$). Earlier experimental work had followed theoretical expectations and assumed pure $p_{1/2}$ for these states, but as seen in Fig. 11, the data are clearly inconsistent with pure $p_{1/2}$ transfer. A reanalysis of the data of Ref. 1 which drops the assumption of pure $p_{1/2}$ transfer shows mixing consistent with our results. Nevertheless, the high degree of mixing deduced is surprising and perhaps due to the collective character of these states.

The $(p_{1/2}^{-1}d_{5/2})$ matrix elements are fully consistent with previous work, whereas for two of the eight

$(p_{3/2}^{-1}d_{5/2})$ matrix elements significant differences with previous values are seen, especially for the $(p_{3/2}^{-1}d_{5/2})3^-$ configuration. The latter comes from the large $p_{3/2}$ component exciting the 6.130-MeV level.

No evidence was found (up to 25-MeV excitation) for the often postulated significant admixture of higher orbitals to the ^{16}O core.

ACKNOWLEDGMENTS

We wish to thank William Temple for his help during data taking. The authors are also indebted to the cyclotron staff of the Indiana University Cyclotron Facility (IUCF) for their cooperation and to W. R. Lozowski for preparing the targets. This work was supported in part by the National Science Foundation.

[1]O. Karban, A. K. Basak, P. M. Lewis, and S. Roman, Phys. Lett. **112B**, 433 (1982).

[2]P. V. Drumm, O. Karban, A. K. Basak, P. M. Lewis, S. Roman, and G. K. Morrison, Nucl. Phys. **A448**, 93 (1986).

[3]Swapan K. Saha, W. W. Daehnick, S. A. Dytman, P. C. Li, J. G. Hardie, G. P. A. Berg, C. C. Foster, W. P. Jones, D. W. Miller, and E. J. Stephenson, Phys. Rev. C **40**, 39 (1989).

[4]W. W. Daehnick, Phys. Rep. **96**, 317 (1983).

[5]R. Mendelson, J. C. Hardy, and J. Cerny, Phys. Lett. **31B**, 126 (1970).

[6]G. Mairle, G. J. Wagner, P. Doll, K. T. Knöpfle, and H. Breuer, Nucl. Phys. **A299**, 39 (1978).

[7]H. Breuer, G. J. Wagner, K. T. Knöpfle, G. Mairle, and P. Doll, Phys. Lett. **96B**, 35 (1980).

[8]G. Mairle, G. J. Wagner, P. Doll, K. T. Knöpfle, H. Riedesel, K. Schindler, G. J. Wagner, V. Bechtold, and L. Friedrich, in Polarization Phenomena in Nuclear Physics, Proceedings of the Fifth International Symposium, Sante Fe, 1980, AIP Conf. Proc. No. 69, edited by G. G. Ohlsen, R. E. Brown, N. Jarmie, W. W. McNaughton, and G. M. Hale (AIP, New York, 1981), p. 685.

[9]B. S. Reehal and B. H. Wildenthal, Part. Nucl. **6**, 137 (1973).

[10]P. W. M. Glaudemans, in *Proceedings of the International Symposium on Nuclear Shell Models,* Drexel University, 1984, edited by M. Vallieres and B. H. Wildenthal (World Scientific, Singapore, 1984), pp. 2–19.

[11]E. J. Stephenson, J. C. Collins, E. C. Foster, D. L. Friesel, W. W. Jacobs, W. P. Jones, M. D. Kaitchuck, P. Schwandt, and W. W. Daehnick, Phys. Rev. C **28**, 134 (1983); see also W. Haeberli, Annu. Rev. Nucl. Sci. **17**, 373 (1967).

[12]G. P. A. Berg, L. C. Bland, B. M. Cox, D. DuPlantis, D. W. Miller, K. Murphy, P. Schwandt, K. A. Solberg, E. J. Stephenson, B. Flanders, and H. Seifert, IUCF Scientific and Technical report, 1986.

[13]F. Ajzenberg-Selove, Nucl. Phys. **A460**, 1 (1986).

[14]J. R. Comfort, fitting code AUTOFT, University of Pittsburgh (unpublished).

[15]W. W. Daehnick, J. D. Childs, and Z. Vrcelj, Phys. Rev. C **21**, 2253 (1980).

[16]P. D. Kunz, University of Colorado (unpublished); J. R. Comfort, FRUCK2:DWBA enhancements and instruction (unpublished).

[17]N. Austern, Nucl. Phys. **A292**, 190 (1977); W. D. M. Rae, Ph. D. Thesis, Oxford University, 1976 (unpublished).

[18]K. F. von Reden, W. W. Daehnick, S. A. Dytman, R. D. Rosa, J. D. Brown, C. C. Foster, W. W. Jacobs, and J. R. Comfort, Phys. Rev. C **32**, 1465 (1985).

[19]I. S. Towner, *A Shell Model Description of Light Nuclei* (Clarendon, Oxford, 1977), p. 293.

[20]W. W. Daehnick, M. J. Spisak, and J. R. Comfort, Phys. Rev. C **23**, 1906 (1981).

[21]J. D. Cossairt, S. B. Talley, D. P. May, R. E. Tribble, and R. L. Spross, Phys. Rev. C **18**, 23 (1978).

[22]P. G. Roos, S. M. Smith, V. K. C. Cheng, G. Tibell, A. A. Cowley, and R. A. Riddle, Nucl. Phys. **A255**, 187 (1975).

[23]M. A. Firestone, J. Jänecke, A. Dudek-Ellis, P. J. Ellis, and T. Engeland, Nucl. Phys. **A258**, 317 (1976).

[24]S. E. Darden, Sudhir Sen, G. Murillo, M. Fernandez, J. Ramirez, A. Galivido, P. L. Jolivette, and B. P. Hichwa, Nucl. Phys. **A429**, 218 (1984).

[25]K. A. Snover, E. G. Adelberger, P. G. Ikossi, and B. A. Brown, Phys. Rev. C **27**, 1837 (1983).

[26]A. P. Zuker, B. Buck, and J. B. McGrory, Phys. Rev. Lett. **21**, 39 (1968).

[27]V. Gillet and N. Vinh Mau, Nucl. Phys. **54**, 321 (1964).

[28]S. T. Hsieh, K. T. Knöpfle, G. Mairle, and G. J. Wagner, Nucl. Phys. **A243**, 380 (1975).

[29]P. J. Ellis and T. Engeland, Nucl. Phys. **A144**, 161 (1970).

[30]G. J. Wagner, K. T. Knöpfle, G. Mairle, P. Doll, and H. Hafner, Phys. Rev. C **16**, 1271 (1977).

[31]R. A. Leavitt, H. C. Evans, G. T. Ewan, H.-B. Mak, R. E. Azuma, C. Rolfs, and K. P. Jackson, Nucl. Phys. **A410**, 93 (1983).